

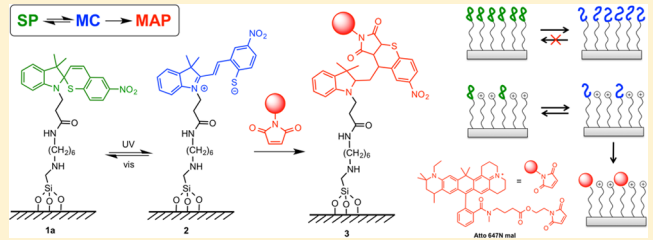
# Effect of Chemical Microenvironment in Spirothiopyran Monolayer Direct-Write Photoresists

Harikrishnan Vijayamohan, Parth Bhide, Dante Boyd, Zhe Zhou, Edmund F. Palermo,<sup>ID</sup> and Chaitanya K. Ullal<sup>\*ID</sup>

Department of Materials Science and Engineering, Rensselaer Polytechnic Institute, 110 8th Street, Troy, New York 12180, United States

## Supporting Information

**ABSTRACT:** We study the effect of the microenvironment on writing chemical patterns into spirothiopyran monolayers over large areas in a single step with light. Surfaces functionalized with photoresponsive spirothiopyran are fabricated by chemically modifying amine-terminated monolayers. The merocyanine isomer selectively participates in a thiol-Michael addition reaction with maleimide-functionalized molecules, rendering these surfaces ideal for fast, mask-less direct writing. The local microenvironment of spirothiopyran is found to strongly influence the kinetics of photoswitching. The quantum yield of ring opening is found to be 17 times faster for spirothiopyran surrounded by a locally charged environment rich in guanidinium diluent molecules as compared to a closed-packed monolayer without diluents. Hydrophilic environments are also found to improve the kinetics of ring closing. Optimization of the diluent concentration leads to dramatic improvements in both contrast and yield of direct writing. This enables the monolayer to be used for maskless two-color photopatterning in which spatial control over patterning is obtained by varying the relative intensity of incident UV and green light. These experiments demonstrate the capacity of spirothiopyran monolayers to serve as a versatile toolbox for rapid, large-area surface functionalization.



## INTRODUCTION

Photopatterning of chemically assembled monolayers to spatially vary surface properties is of interest in diverse applications like organic electronic devices, sensors, synthetic biology, and drug delivery.<sup>1–4</sup> Photopatternable monolayers have typically been prepared either by thiol-based self-assembly or silane-based covalent attachment on metal or silicon dioxide-based substrates.<sup>2,4–8</sup> Such photopatterning is carried out by deep UV ( $\sim 250$  nm) induced selective area photooxidation or bond breaking, with the monolayer functioning as a photoresist.<sup>6,8,9</sup> The multiple processing steps of etching, rinsing, postdevelopment functionalization, etc. are viewed as being onerous but unavoidable<sup>10</sup> relative to one-step direct writing. This is particularly true while patterning biomolecules that degrade upon exposure to deep UV wavelengths. These wavelengths also introduce defects by degradation of the monolayer.<sup>11,12</sup> Recently, one-step solution-based monolayer patterning techniques that use a more biomolecule friendly 365 nm UV light to yield defect-free patterns over large areas have been demonstrated. The resolution of these methods is, however, compromised by refraction of light<sup>13</sup> and diffusion<sup>12</sup> in solution, respectively. Here, we present a complementary method based on the use of spirothiopyran (STP) photochromic switches that do not face these limitations and tackle the key issue of contrast that arises in the use of such molecules as direct write resists.

Photochromic molecules are an attractive material system to create tunable surfaces due to the light-driven reversible conversion between constituent isomers.<sup>14</sup> Of the different classes of photochromic molecules, spiropyran has been extensively examined due to the high degree of contrast in physical and chemical properties of its isomers.<sup>15</sup> Spiropyran switches from its spiro form (SP) to a merocyanine isomer (MC) when illuminated with soft-UV/blue (365–410 nm) light. The MC can exist in a neutral quinoidal form or a charge-separated zwitterionic form, which can undergo a ring-closing reaction to reconstitute to SP when illuminated with visible light. Spiropyran has been covalently attached to metal<sup>16,17</sup> or glass<sup>18,19</sup> substrates to form photoactivatable surfaces for a variety of applications including sensors,<sup>20,21</sup> electrodes,<sup>22–26</sup> photocontrolled transport channels,<sup>27–29</sup> and surface receptors.<sup>30,31</sup> The photoactivatable responses of such surfaces utilize shifting the  $SP \rightleftharpoons MC$  equilibrium toward one distinct isomer by shining UV or visible light, respectively.

Despite their success in photoactivatable surfaces, spiropyran monolayers are not suited for direct writing. Garcia et al.<sup>32</sup> have examined how the isomerization of spiropyran monolayers depends on solvent polarity and microenvironment and showed that even after optimizing the local microenvironment,

Received: September 28, 2018

Revised: February 21, 2019

Published: February 26, 2019

only 10–20% of the spiropyran molecules reversibly isomerize upon illumination.<sup>19,33</sup> This lowers the contrast of the switchable response; the change in contact angle for water on flat substrates was only  $\sim 10^\circ$ .<sup>34</sup> A second hurdle is the lack of a permanent irreversible “direct written” state. Currently, spiropyran monolayers suffer from photofatigue, which limits the number of usable switching cycles.<sup>15</sup>

In this paper, we demonstrate monolayers of the sulfur-containing analogue, spirothiopyran (STP), a molecule that has attracted recent attention,<sup>35–38</sup> as a viable alternative for direct writing. The MC isomer of STP can participate in a thiol-Michael addition with  $\alpha$ ,  $\beta$  unsaturated carbonyl compounds to form a nonswitchable Michael addition product (MAP), which serves as the desired written state. We have previously shown that the unique  $SP \rightleftharpoons MC \rightarrow MAP$  kinetics allows the spirothiopyran-maleimide material system to be used for lithography by using a photomask as well as for maskless two-color photopatterning in which spatial control over patterning can be modulated by the UV–visible light intensity ratio.<sup>39</sup>

To demonstrate the use of STP monolayers as a direct write resist, first, covalent attachment of an STP derivative to a molecular monolayer is performed by standard synthetic procedures. Then, flood illumination of UV and a standing wave of green light enables spatial patterning of the open and closed form within the monolayer (Figure 1). In the closed

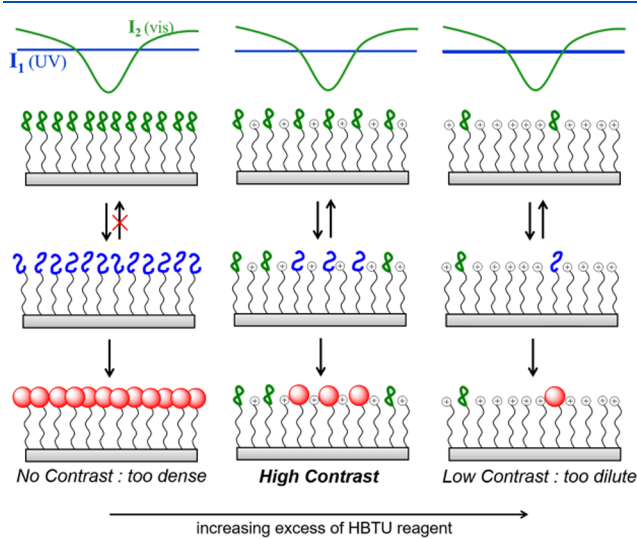


**Figure 1.** Green-induced ring-closing reaction is suppressed when the surface grafting density of SP is high. When diluted in a microenvironment of cationic charge, the switching becomes facile.

form, the STP molecule is inert, whereas in the open form, the thiolate anion reacts readily with maleimides (Figure 2a). Thus, a maleimide-functionalized fluorescence dye, Atto 647N, is selectively attached to the monolayer only in the areas where the open form predominates. This method has the potential to enable large area maskless lithography, in principle. In practice, it is necessary to finely tune the equilibrium between the chemical species involved.

To that end, we functionalized a silica surface with an amino-functionalized silane and coupled the amines to a spirothiopyran derivative bearing a carboxylic acid (STP-COOH, 4, Scheme 1) by means of activated ester. We employed HBTU, a common coupling reagent in peptide

chemistry.<sup>40</sup> This reagent is normally used in a 1:1 stoichiometric equivalent with the carboxylate to avoid the typically undesired side reaction of HBTU with amines, the latter generating a guanidinium side product that is inert to coupling. In this work, we hypothesized that the inclusion of excess HBTU, and thus intentional formation of the guanidine side product to varying extents, would provide a convenient one-pot approach to finely tune the microenvironment surrounding the STP molecules in the monolayer. Because the photochromic switching equilibrium is highly sensitive to the polarity of the media, we reasoned that adjusting the surface concentration of guanidinium, relative to STP, would enable control of the resulting lithographic contrast. Indeed, we found that one stoichiometric equivalent of HBTU to STP-COOH yielded a high density of STP on the surface. However, this high density of STP creates a nonpolar environment that disfavors switching from the open merocyanine form to the closed STP form. As a result, Atto 647N dye attaches to the surface in a homogeneous manner, regardless of the two-color pattern, and thus negligible contrast is observed. Excitingly, as the equivalents of HBTU (in excess of 1) are gradually increased, the achievable contrast continuously increases, reaching a maximum at the ratio of 1:7::STP/HBTU. When the excess of HBTU is increased still further, the total fluorescence signal and contrast obtained begins to decrease because the STP molecules on the surface become highly diluted (Figure 1). Thus, we discovered that tuning the reaction conditions for the formation of the monolayer (simply by adjusting the ratio of carboxylic acid to coupling reagent) enables a rapid and facile route to optimize contrast of patterning. An optimized guanidinium microenvironment was found to improve the kinetics of bidirectional photoswitching in spirothiopyran with the rate of ring opening increasing by a factor of 17. Furthermore, a local hydrophilic environment was demonstrated to be much more effective at photokinetic enhancement as compared to a nonpolar hydrophobic environment.

## EXPERIMENTAL SECTION

**Materials.** Reagents and chemicals were purchased from Sigma-Aldrich and used without further purification. *N*-(6-Aminohexyl)-aminomethyltriethoxysilane was purchased from Gelest. Atto 647N maleimide was purchased from Atto-Tec GmbH.

**Instrumentation.** Proton ( $^1H$ ) and carbon ( $^{13}C$ ) NMR spectra were recorded on a Bruker SB 800 MHz spectrometer. Electrospray ionization/mass spectroscopy analysis was carried out using a Thermo Scientific LTQ Orbitrap XL Hybrid Ion Trap-Orbitrap Mass Spectrometer. X-ray photoelectron spectroscopy (XPS) measurements were carried out on a PHI Versaprobe 5000 scanning system. Atomic force microscope (AFM) analysis was carried out on a Digital Instruments Multimode IIIa Atomic Force Microscope. Attenuated total reflectance-Fourier transform infrared (ATR-FTIR) measurements were performed using a Biorad-Excalibur FTIR spectrometer. Confocal microscopy measurements were carried out using an in-house built stimulated emission depletion (STED) system utilizing a Picquant LDH DC 640 laser for excitation, MPB PRFL-P-30-775-B1R laser for depletion and a SPCM-AQRH-13-FC Excelitas single-photon counting module for detection.

**Synthesis.** Carboxylic acid functionalized spirothiopyran (4, Scheme 1) was synthesized by previously reported procedures with minor modifications.<sup>37,41</sup> Details of the synthetic route are given in the Supporting Information (SI).

**Synthesis of Spirothiopyran-Functionalized Monolayers (1a).** Amine functionalized glass surfaces were prepared by a well-established protocol specifically designed to yield hydrolysis-resistant

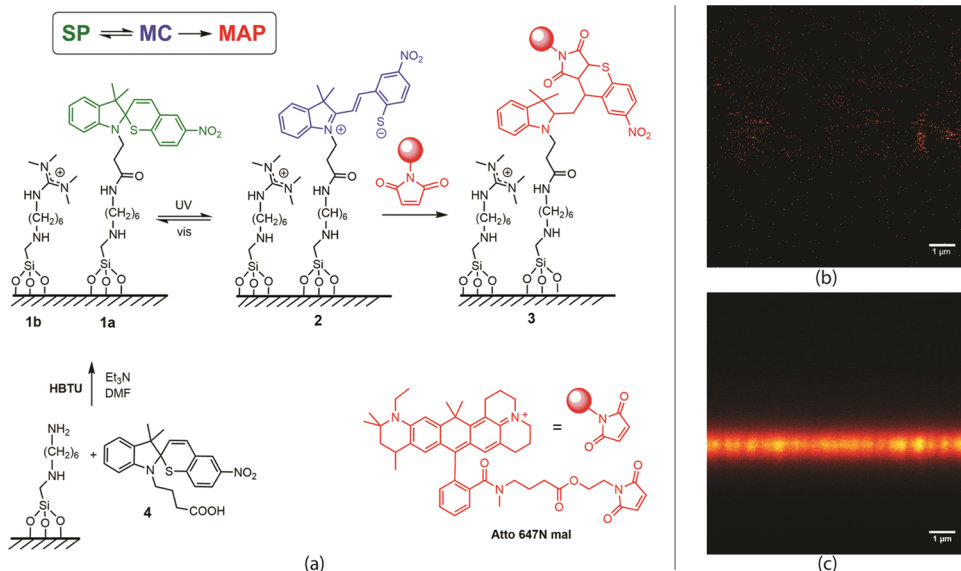
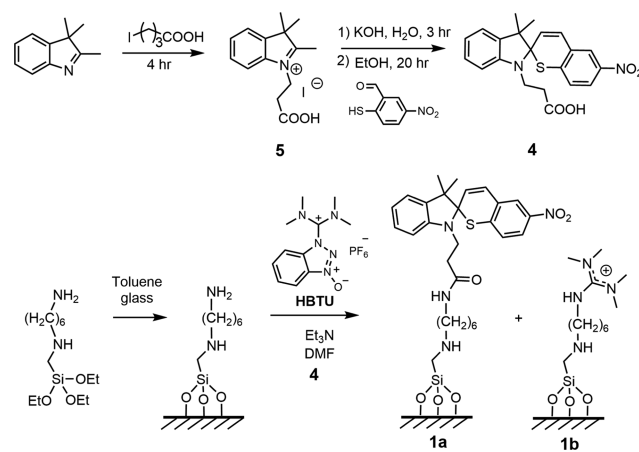


**Figure 2.** (a) Scheme illustrating photochromic switching in spirothiopyran. The merocyanine isomer can participate in a thiol-Michael addition with maleimide-functionalized compounds. Also shown are XZ-confocal microscopy images of the spirothiopyran monolayer prepared using a 1:7 SPT/HBTU molar feed ratio after reacting with the Atto maleimide dye before (b) and after (c) UV exposure.

**Scheme 1. Scheme Depicting Synthetic Route to Carboxylic Acid-Functionalized Spirothiopyran and Spirothiopyran-Functionalized Monolayers (STP-ML)**



monolayers.<sup>42</sup> Glass coverslips were cleaned by immersing in freshly prepared piranha solution (7 parts concentrated sulfuric and 3 parts 30% hydrogen peroxide) for 30 min. (Caution: Piranha solution reacts violently with organic matter.) The coverslips were removed and then rinsed twice with deionized water and dried in a clean oven at 140 °C for 45 min. Amine-functionalized monolayers were synthesized by immersing the cleaned glass coverslips in a 2% by volume *N*-(6-aminohexyl)aminomethyltriethoxysilane solution in anhydrous toluene at 70 °C under nitrogen atmosphere for 1 h. The coverslips were then rinsed twice with toluene, ethanol, and water and dried at 140 °C for 60 min.

A 3.97 mg of STP-COOH (.01 mmol) (4) was mixed with the desired quantity of HBTU in 10 mL of anhydrous dimethylformamide (DMF) and stirred for 5 min. The resulting mixture was introduced to the amine-functionalized coverslips, followed by the addition of 5  $\mu\text{L}$  of anhydrous triethylamine to the reaction mixture. After 16 h, the coverslips were removed and thoroughly washed with acetone and ethanol and then dried in air.

**UV Photopatterning and Characterization.** Fifty microliters of an 8  $\mu\text{M}$  solution of Atto 647N maleimide in DMF was dropcast between the spirothiopyran monolayer and a microscope slide with a

125  $\mu\text{m}$  spacer in between (Grace Bio Labs GBL654002). This assembly was exposed to UV light of intensity 0.8  $\text{mW}/\text{cm}^2$  for 15 min. STP-ML was then extracted from the spacer and washed in methanol for 30 min. After drying the coverslip in air, 10  $\mu\text{L}$  of a 97% thiidiethanol (TDE) in water solution was used to mount the monolayer for confocal imaging. The excitation intensity at the back focal plane of the objective lens was recorded as 11.2  $\text{mW}/\text{cm}^2$ .

**Two-Color Photopatterning.** Spirothiopyran monolayer-dye assembly described above was exposed to a standing wave of green (Coherent Verdi V2 laser, 50  $\text{mW}/\text{cm}^2$  intensity) and a plane wave of UV (Thorlabs M365LP1 LED, 10  $\text{mW}/\text{cm}^2$  intensity) using a Lloyds mirror setup. Optical power was measured using a Coherent LabMAX-TO power meter with an LM-2 VIS Silicon optical sensor. After 4 min of exposure, the monolayer samples were washed in methanol for 30 min and after drying, mounted in 10  $\mu\text{L}$  of a 97% TDE solution for confocal imaging. Photographs of the experimental setup are given in the SI.

## RESULTS AND DISCUSSION

It is well known that HBTU provides excellent yield for amide coupling, but due to its tendency to react with amines to form a guanidinium side product, the concentration, order, and timing of the reaction for amide coupling are essential.<sup>43</sup> To synthesize a dense, uniform monolayer of spirothiopyran via covalent attachment, HBTU is taken in a molar ratio slightly lower than one with respect to the carboxylic acid (Scheme 1), and a preactivation mixture of the carboxylic acid functionalized spirothiopyran and HBTU is required to be prepared before introducing the amine-functionalized glass surfaces.<sup>40</sup> Use of an HBTU/STP molar feed ratio greater than 1 introduces excess guanidine diluent molecules among the amide-coupled spirothiopyran, on average proportional to the feed ratio used during the synthesis (Figure 2a). We utilized this as an effective means to control the microenvironment of the anchored photochromes (the formation of guanidine moieties due to excess HBTU during amide coupling is confirmed by ATR-FTIR measurements, see the Supporting Information).

Figure 3a–c shows the Si 2p, N 1s, and S 2s XPS spectra taken at different stages of the monolayer synthesis. As

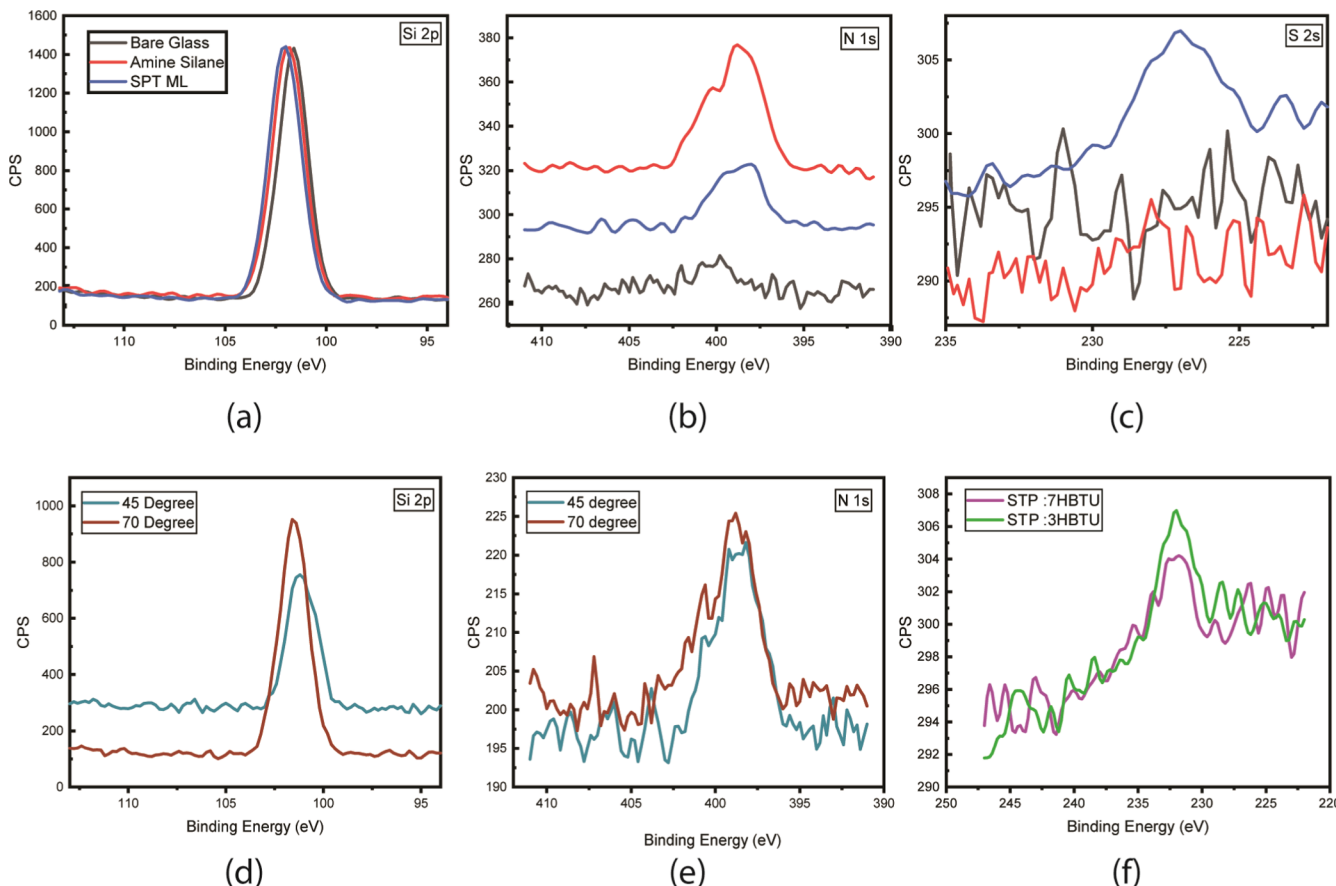


**Figure 3.** XPS spectra of (a) Si 2p, (b) N 1s, and (c) S 2s peaks for the bare glass substrate, amine-functionalized monolayer, and subsequent covalently attached spirothiopyran samples prepared using a 1:3 STP/HBTU feed ratio. Angle-resolved (AR)-XPS spectra of (d) Si 2p and (e) N 1s for STP monolayers prepared using a 1:7 HBTU molar feed ratio analyzed at 45 and 70° take-off angles (TOA). (f) S 2s XPS spectra for the samples prepared using two different STP/HBTU molar feed ratios.

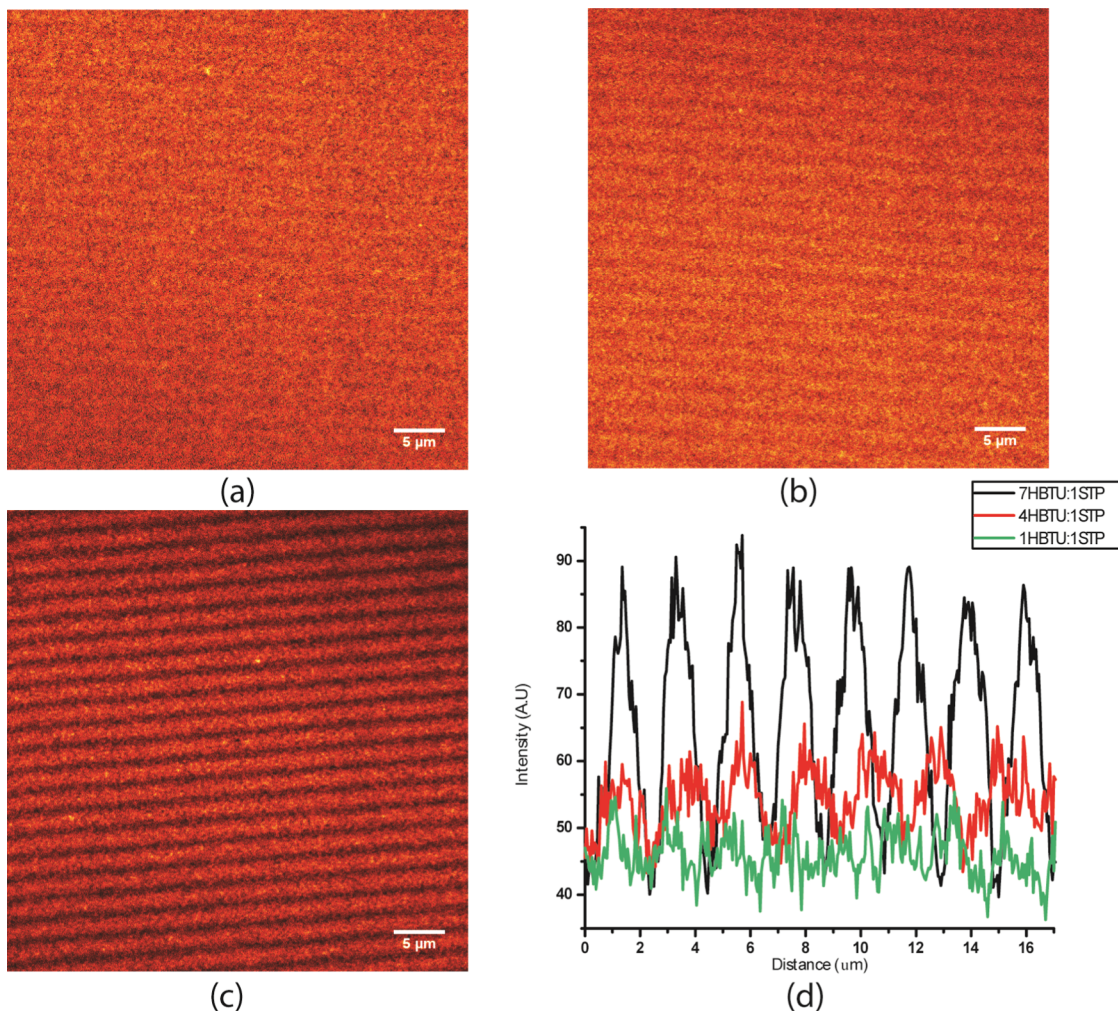
expected, the clean bare glass substrate gives a good signal only for the Si 2p photoelectrons; an N 1s peak is detected after covalently attaching the amine-terminated silane and an S 2s peak is seen only after the subsequent amide coupling with spirothiopyran. We note the fact that the MC isomer lifetime (minutes)<sup>39</sup> is much shorter than the XPS data collection time (~6 h). This longer collection is necessitated by the vanishingly low concentration of the surface-bound spirothiopyran, which prevents recording of a separate XPS spectra for the MC isomer. The presence of spirothiopyran after amide coupling is also confirmed by utilizing the selective reaction of the MC isomer with maleimide-functionalized Atto dye (Figure 2a). Figure 2b,c shows the confocal microscopy images of the spirothiopyran monolayers before and after UV exposure when kept exposed to an Atto maleimide dye solution. A uniform bright signal over a single point spread function depth confirms the covalent attachment of the Michael addition product of the dye to spirothiopyran.

Figure 3d,e shows the Si 2p and N 1s angle-resolved (AR)-XPS spectra for the spirothiopyran monolayer taken at 45 and 70° take-off angles (TOA). Increasing the take-off angle allows the X-ray beam to probe larger sample depths from 2 to 3 nm (45° TOA) to 7–10 nm (70° TOA).<sup>44</sup> Increasing the TOA is found to augment the detected photoelectron peak intensity for Si 2p but decreases the N 1s peak intensity, thus confirming that our sample is confined to depths of at most a few nm. Depth profiling using (AR)-XPS on the amine functionalized

surfaces allowed us to calculate a thickness of 1 nm for our amine-functionalized surfaces, consistent with previously reported studies<sup>42,45</sup> (details provided in the Supporting Information).

Figure 3f shows the S 2s XPS spectra of two samples prepared for two different STP/HBTU molar feed ratios. The areas under the peaks are found to be in the ratio of 1:2.3, which is proportional to the 1:3 ratio expected from the feed ratios taken in a solution. Given the qualitative nature of such XPS results, we refer to the composition of the surface in terms of the molar feed ratios taken in a solution. Finally, the relative homogeneity of the covalently modified surfaces was confirmed using atomic force microscopy (see the Supporting Information).

The unique chemistry of the spirothiopyran photochromes allows them to be readily used for fast, phototriggered one-step surface patterning with maleimide-functionalized molecules when exposed to UV light. Furthermore, utilizing the MC → SP ring-closing isomerization, the Michael addition reaction can be photoinhibited at a relatively low visible light intensity.<sup>39</sup> This allows us to use the STP-ML for maskless large area patterning using a two-color writing setup. Briefly, when STP-ML is under simultaneous illumination of UV (which induces the SP isomer to switch to MC) and green (which induces the MC isomer to switch back to STP), a higher intensity of green will force the photochromic system to remain in its unreactive STP isomer. Hence, spatial control



**Figure 4.** Confocal images of spirothiopyran monolayer after two-color patterning with Atto 647N maleimide dye as per the scheme shown in Figure 1. Images shown are for the samples with the following compositions: (a) monolayer with no diluent molecules, (b) monolayer prepared using a 1:4 spirothiopyran/HBTU molar feed ratio, and (c) monolayer prepared using a 1:7 spirothiopyran/HBTU molar feed ratio. (d) Line profile comparing images in (a)–(c).

over patterning can be obtained by selectively introducing minima/zeros for green illumination.<sup>46</sup> The feature size of the resulting pattern can also be tuned by controlling the relative intensity of the visible to UV light incident.

To this effect, we designed a writing system, where the STP-ML in the presence of an Atto maleimide dye solution was simultaneously exposed to a floodlit illumination of UV and a standing wave of green. Writing, by formation of the Michael addition product of the maleimide dye with merocyanine (Figure 2a), is expected to occur only at the nodes of the green standing wave. However, when patterning was carried out on STP-ML prepared using a 1:1 STP/HBTU molar feed ratio, the contrast of the 1D lines obtained was very poor (Figure 4a); patterning was found to occur nearly uniformly across the green standing wave. To study the effect of the chemical microenvironment of spirothiopyran on the two-color writing response, samples prepared with increasing STP/HBTU molar feed ratios were utilized for patterning with the same exposure conditions. Introducing guanidinium diluents on the STP surfaces were found to drastically improve the fluorescence yield and contrast of the 1D lines obtained (Figure 4a,b). For 1:7 STP/HBTU molar feed ratio taken during the synthesis, the contrast and signal of the lines formed are maximized, with

clear zeros visible (Figure 4c,d). Further increasing the relative molar feed ratio of HBTU was found to decrease the net yield and contrast of the lines obtained as the monolayer surface becomes increasingly dilute with respect to the STP surface density.

To further explore the role of the microenvironment on direct writing using STP-ML, the Michael addition product concentration (3, Figure 2) can be quantified by measuring the emitted fluorescence photon count from the Atto dye covalently attached to the monolayer when exposed to only UV light. Samples prepared with different SPT/HBTU feed ratios were exposed to an 8  $\mu$ M Atto 647N maleimide dye solution under 0.8 mW/cm<sup>2</sup> UV exposure for 15 min (see **Experimental Section** for details). Contrasts were determined against control samples kept in the dark. For SPT-ML with no diluent molecules (1:1 feed ratio), the contrast between the control sample and the test sample was small (2.4 $\times$  increase). The high fluorescence signal detected for the control sample indicates that a substantial proportion of spirothiopyran molecules are already present in the merocyanine isomer form in the dark. This behavior is contrary to what is seen for spirothiopyran in a solution,<sup>39</sup> we suspect a stabilizing dipole–dipole interaction between charge-separated merocyanine

isomers in a tightly packed monolayer to be responsible for this effect. Upon increasing the molar feed ratio of HBTU to STP-COOH, the total fluorescence yield and the contrast between the control and test samples dramatically increased (Figure 5).

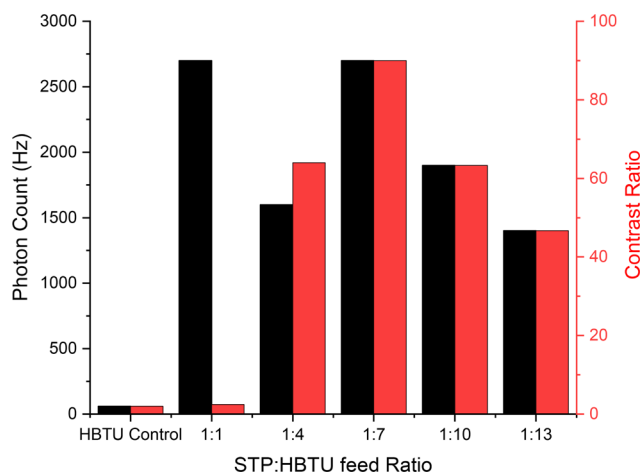


**Figure 5.** Impact of varying STP/HBTU molar feed ratio during the synthesis on photopatterning yield and contrast of the resultant monolayers. Photon count (Hz) is the number of fluorescent photons detected per second by the avalanche photodiode detector of our confocal microscope. Contrast is maximized when the STP molecules are optimally diluted in a microenvironment of cationic charge.

The yield and contrast are seen to pass through a maxima before subsequently decreasing. The addition of diluent molecules causes the spirothiopyran molecules to remain in the spiro-isomer form in the dark, which markedly lowers the control sample signal. Furthermore, the increase in detected fluorescence yield can be ascribed to faster ring opening kinetics in samples with higher diluent concentrations. Guanidinium diluents (**1b**, Scheme 1) provide a local polar chemical environment for the spirothiopyran molecules when compared to a closely packed spiro-isomer assembly. An improvement in contrast upon the introduction of diluent molecules has been observed before for spiropyran monolayers;<sup>18</sup> however, unlike spiropyran, where the increase in contrast obtained due to shifting the  $[MC]/[SP]$  equilibrium constant is marginal at best, the addition of the  $MC \rightarrow MAP$  step perturbs the photochromic switching away from equilibrium, leading to 2 orders of magnitude improvement in the signal. Hence, a spirothiopyran monolayer with guanidinium diluents serves as an excellent photoswitchable surface where desired areas of interest can be activated and patterned using UV light.

A closer examination of the signal obtained from maleimide patterning reveals an interesting observation regarding the kinetics of photoswitching. For the  $SP \rightleftharpoons MC \rightarrow MAP$  reaction carried out in dark under UV illumination with no visible light present, we can ignore the  $MC \rightarrow SP$  photodriven ring closing, and as the exposure is carried out at room temp, we can also ignore the thermal back-isomerization. Hence, the evolution of MAP as a function of time can be modeled as a series of sequential reactions ( $SP \rightarrow MC \rightarrow MAP$ ), with the concentration of the Michael addition product as a function of time calculated to be

$$[MAP] = [SP]_0 \left( 1 - \frac{1}{k_2 - k_1} (k_2 e^{-k_1 t} - k_1 e^{-k_2 t}) \right) \quad (1)$$

where  $k_1$  is the rate constant for the UV-induced ring opening of spirothiopyran into merocyanine,  $k_2$  ( $= [Atto - Mal]k_{MA}$ ) is the pseudo-first-order rate constant for the thiol-Michael addition with the Atto maleimide dye and  $[SP]_0$  is the initial concentration of spirothiopyran (in the spiro form) on the monolayer. Due to the much higher concentration of Atto maleimide as compared to spirothiopyran and the low intensity of UV light used, we can consider the ring-opening reaction to be the rate-determining step ( $k_2 \gg k_1$ ) and simplify the above expression to

$$[MAP] = [SP]_0 (1 - (e^{-k_1 t})) \quad (2)$$

For the data in Figure 5, across different STP/HBTU molar feed ratios, the UV intensity and time of exposure were kept constant. Also, during confocal measurements, as the quantum yield of the Atto maleimide dye will not vary across samples and the excitation intensity and detection conditions remain constant, we can assume the photon count recorded to be directly proportional to the concentration of the Michael addition product. Hence, using eq 2, assuming the spirothiopyran density among the different monolayer samples is in the same ratio as the molar feed ratio taken during the synthesis, we can calculate the ratio of the UV-induced ring-opening rate constants ( $k_1$ ) for different monolayer samples. The rate constants normalized with respect to the monolayer without diluent molecules is plotted as a function of composition in Figure 6. The rate constant for ring-opening

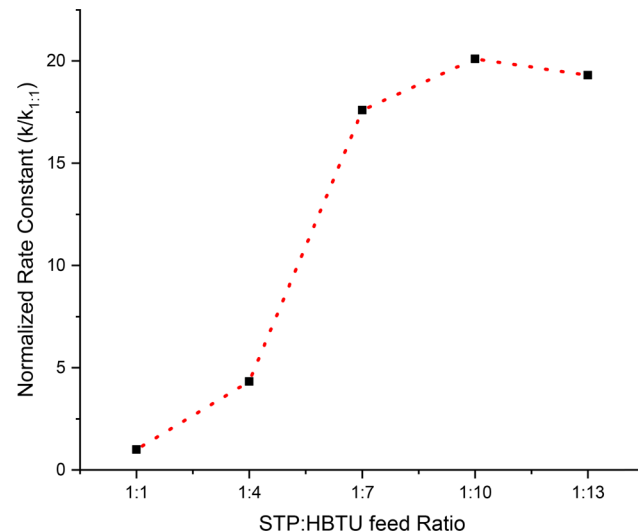


**Figure 6.** Plot of normalized ring opening rate constant as a function of monolayer composition. The rate constants saturate with increasing guanidinium concentration. The dotted lines are guide to the eye.

shows a rapid increase with increasing guanidinium diluent concentration and saturates. The kinetics of photoisomerization of spirothiopyran have been studied before<sup>39</sup> and are dependent on the intensity of UV light, molar extinction coefficient of the spiro-isomer, and the quantum yield of ring opening. As the UV intensity is same across different samples and the extinction coefficient is also expected to remain constant, the faster rate constants of ring opening can be ascribed to the differential quantum yields. The quantum yield

for ring opening for spirothiopyran prepared using a 1:10 STP/HBTU feed ratio is nearly 17 times higher than a 1:1 feed ratio (no diluent molecules). The faster kinetics of the ring opening could probably arise due to a hydrophilic local chemical environment created by the guanidinium molecules (**1b**, Scheme 1). A similar enhancement in the quantum yield of isomerization was reported recently for spiropyran molecules trapped in bile salts aggregates, with increased quantum yields determined for molecules trapped in polar environments.<sup>47</sup> Our results here for the spirothiopyran monolayer follow the same trend, with the increased quantum yield of ring opening manifesting as higher contrast and yield for thiol-Michael addition surface patterning. Thus, our dye-tagging experiments show that the chemical microenvironment significantly influences the kinetics of spiropyran to merocyanine isomerization, which acts as the critical rate-determining step for the overall writing system.<sup>48</sup> The high rate constants of Michael addition between the thiol merocyanine isomer and the maleimide molecules renders the reaction independent of changes in the microenvironment.<sup>49</sup>

Further support for this hypothesis is obtained by changing the identity of the diluent molecules. To illustrate the importance of the polarity of the diluent molecule, the samples were prepared with decanoic acid (DA) and 1-(3-carboxypropyl)-2,3,3-trimethyl-3H-indol-1-ium iodide (IA) using a 7:1 molar feed ratio with respect to STP-COOH. As seen in Figure 7, DA amide as a diluent gives a much lower yield for

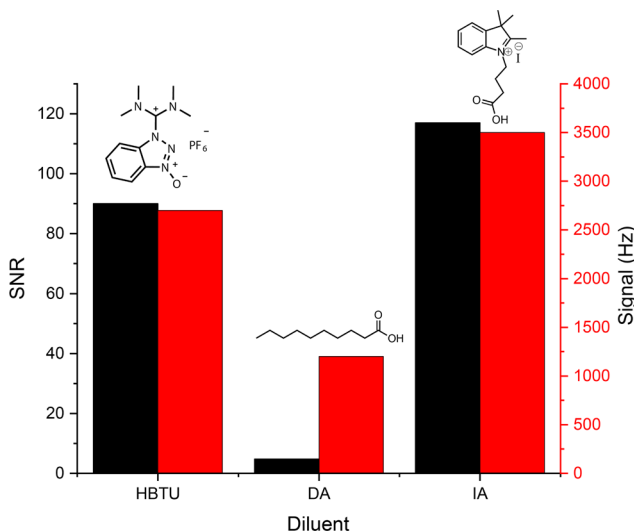


**Figure 7.** Impact of varying diluent composition on contrast (signal-to-noise ratio) and total signal. Photon count (Hz) is the number of fluorescent photons detected per second in the avalanche photodiode detector of the confocal microscope.

patterning as well as poorer contrast when compared to guanidinium, whereas the IA amide diluent is seen to give better performance than guanidinium (better conformational steric effects may contribute to this enhancement). Thus, it is essential to optimize the concentration and choice of the correct diluent molecule for improving both the contrast of writing and the yield of the final product. Additionally, as compared to spiropyran monolayers, since the Michael addition product is in a permanently modified nonswitchable state, photopatterning of spirothiopyran can create indelible features not affected by photofatigue.

As compared to the rate of ring opening, it is difficult to quantify the effect of the chemical microenvironment on the kinetics of photoinduced ring closing. Using a monolayer for patterning makes it extremely difficult to directly measure the concentration of the unreacted STP molecules using spectroscopic techniques. However, the increase in contrast of two-color patterning with increasing HBTU molar feed ratios (Figure 4d) clearly demonstrates that for the same intensities of green light, a high diluent concentration of guanidine is more efficient for inhibition and hence for the photodriven MC  $\rightarrow$  SP ring-closing reaction. Thus, we can infer that the quantum yield of both forward and reverse isomerizations is found to be highly sensitive to the microenvironment of the covalently attached spirothiopyran.

The saturation of the ring-opening rate constant for higher molar feed ratio, coupled with the detrimental effect on both the yield and contrast of patterning due to the decreasing density of covalently attached spirothiopyran with increasing HBTU molar feed ratios, means that there is a clear trade-off between the net intensity and contrast of photopatterns that can be fabricated against the density of spirothiopyran photochromes on the surface. Photoinhibition during two-color patterning happens within seconds due to high intensity of green used. Photoactivation and the resultant dye tagging were found to saturate within 4–5 min for 10 mW/cm<sup>2</sup> of UV intensity. The overall writing time is determined by the light sources used; it can be further shortened by increasing the exposure intensities. The full width at half-maximum of the resulting lines obtained can be controlled using the intensity of UV and green and can in principle be extended for large area 1D nanopatterning with subdiffraction resolution. We are currently following up by exploring these techniques in our laboratories.

## CONCLUSIONS

Spirothiopyran-functionalized monolayers on glass surfaces were fabricated and characterized by different techniques including XPS, AFM, and confocal microscopy. The ability of the merocyanine isomer to participate in a thiol-Michael addition with  $\alpha, \beta$  unsaturated compounds, perturbing the photoequilibrium between the SP and MC isomer, makes spirothiopyran monolayers excellent candidates for maskless direct writing. The effect of the local chemical environment on the kinetics of writing were explored and the introduction of polar nearest neighbors for the covalently bound spirothiopyran was found to dramatically improve both the contrast and yield of photopatterning. Spirothiopyran monolayers with guanidine diluents prepared using a 1:10 molar feed ratio between STP and HBTU during amide coupling were found to exhibit 17 times higher quantum yield of ring opening as compared to monolayers bereft of any diluent molecules. The polar local environment also improves the rate of photoisomerization of the merocyanine isomer to its spiro form. This enables the spirothiopyran monolayer to be used for two-color photopatterning where writing only occurs at the intensity minima of the visible light. These experiments demonstrate that effective optimization of the local chemical environment allows spirothiopyran monolayers to be a powerful photo-switchable functional surface capable of direct writing with maleimide-functionalized molecules, a feature that makes it very appealing for a multitude of applications.

## ■ ASSOCIATED CONTENT

### ■ Supporting Information

The Supporting Information is available free of charge on the ACS Publications website at DOI: [10.1021/acs.langmuir.8b03304](https://doi.org/10.1021/acs.langmuir.8b03304).

Details of STP-COOH synthesis, XPS depth-profiling calculations, AFM and STED characterizations of STP monolayer surfaces, ATR-FTIR spectra of guanidine-functionalized surface and photographs of the experimental setup for two-color photopatterning ([PDF](#))

## ■ AUTHOR INFORMATION

### Corresponding Author

\*E-mail: [ullalc@rpi.edu](mailto:ullalc@rpi.edu).

### ORCID

Edmund F. Palermo: [0000-0003-3656-787X](https://orcid.org/0000-0003-3656-787X)

Chaitanya K. Ullal: [0000-0002-7178-897X](https://orcid.org/0000-0002-7178-897X)

### Author Contributions

The manuscript was written through contributions of all authors. All authors have given approval to the final version of the manuscript.

### Notes

The authors declare no competing financial interest.

## ■ ACKNOWLEDGMENTS

The authors would like to thank Dr Chang Ryu and Dr Peter Dinolfo for graciously allowing us usage of their laboratory facilities, Rob Planty, Dr Dustin Andersen, and Bryant Colwill for help with characterization, and Dr Liping Huang for access to her Coherent Verdi V2 laser. This work was supported in part by the Engineering Research Centers Program of the National Science Foundation under NSF Cooperative Agreement No. EEC-0812056 and in part by New York State under NYSTAR contract C130145. This work is based in part upon work supported by the National Science Foundation under Grant no. 1610783. This work made use of a Leica STED TCS SP8 3X instrument that was acquired through support from the National Science Foundation (Grant no. NSF-MRI-1725984), with additional support from NYCAP. This work was supported in part by the Ferguson Fellowship through the Department of Materials Science and Engineering at Rensselaer Polytechnic Institute.

## ■ ABBREVIATIONS

STP, spirothiopyran; SP, spiropyran isomer; MC, merocyanine isomer; MAP, Michael addition product; STED, stimulated emission depletion microscopy; NMR, nuclear magnetic resonance; HBTU, *N,N,N',N'*-Tetramethyl-O-(1H-benzotriazol-1-yl) uroniumhexafluorophosphate

## ■ REFERENCES

- (1) Schmaltz, T.; Sforazzini, G.; Reichert, T.; Frauenrath, H. Self-Assembled Monolayers as Patterning Tool for Organic Electronic Devices. *Adv. Mater.* **2017**, *29*, No. 1605286.
- (2) Ni, L.; Dietlin, C.; Chemtob, A.; Croutxé-Barghorn, C.; Brendlé, J. Hydrophilic/Hydrophobic Film Patterning by Photodegradation of Self-Assembled Alkylsilane Multilayers and Its Applications. *Langmuir* **2014**, *30*, 10118–10126.
- (3) Adams, J.; Tizazu, G.; Janusz, S.; Brueck, S. R. J.; Lopez, G. P.; Leggett, G. J. Large-Area Nanopatterning of Self-Assembled Monolayers of Alkanethiolates by Interferometric Lithography. *Langmuir* **2010**, *26*, 13600–13606.

(4) El Muslemany, K. M.; Twite, A. A.; ElSohly, A. M.; Obermeyer, A. C.; Mathies, R. A.; Francis, M. B. Photoactivated Bioconjugation Between Ortho-Azidophenols and Anilines: A Facile Approach to Biomolecular Photopatterning. *J. Am. Chem. Soc.* **2014**, *136*, 12600–12606.

(5) Mowery, M. D.; Smith, A. C.; Evans, C. E. Polydiacetylene Monolayers as Versatile Photoresists for Interfacial Patterning. *Langmuir* **2000**, *16*, 5998–6003.

(6) Herzer, N.; Hoeppener, S.; Schubert, U. S. Fabrication of Patterned Silane Based Self-Assembled Monolayers by Photolithography and Surface Reactions on Silicon-Oxide Substrates. *Chem. Commun.* **2010**, *46*, 5634–5652.

(7) Ni, L.; Chemtob, A.; Croutxé-Barghorn, C.; Brendlé, J.; Vidal, L.; Rigolet, S. Photopatterning of Multilayer n-Alkylsilane Films. *Langmuir* **2012**, *28*, 7129–7133.

(8) See, E. M.; Peck, C. L.; Guo, X.; Santos, W.; Robinson, H. D. Plasmon-Induced Photoreaction of o-Nitrobenzyl-Based Ligands under 550 Nm Light. *J. Phys. Chem. C* **2017**, *121*, 13114–13124.

(9) Huang, J.; Dahlgren, D. A.; Hemminger, J. C. Photopatterning of Self-Assembled Alkanethiolate Monolayers on Gold: A Simple Monolayer Photoresist Utilizing Aqueous Chemistry. *Langmuir* **1994**, *10*, 626–628.

(10) Mostegel, F. H.; Ducker, R. E.; Rieger, P. H.; El Zubir, O.; Xia, S.; Radl, S. V.; Edler, M.; Cartron, M. L.; Hunter, C. N.; Leggett, G. J.; et al. Versatile Thiol-Based Reactions for Micrometer- and Nanometer-Scale Photopatterning of Polymers and Biomolecules. *J. Mater. Chem. B* **2015**, *3*, 4431–4438.

(11) Leuschel, B.; Gwiazda, A.; Heni, W.; Diot, F.; Yu, S.-Y.; Bidaud, C.; Vonna, L.; Ponche, A.; Haidara, H.; Soppera, O. Deep-UV Photoinduced Chemical Patterning at the Micro- and Nanoscale for Directed Self-Assembly. *Sci. Rep.* **2018**, *8*, No. 10444.

(12) Williams, M. G.; Teplyakov, A. V. Indirect Photopatterning of Functionalized Organic Monolayers via Copper-Catalyzed “Click Chemistry”. *Appl. Surf. Sci.* **2018**, *447*, 535–541.

(13) Pester, C. W.; Narupai, B.; Mattson, K. M.; Bothman, D. P.; Klinger, D.; Lee, K. W.; Discekici, E. H.; Hawker, C. J. Engineering Surfaces through Sequential Stop-Flow Photopatterning. *Adv. Mater.* **2016**, *28*, 9292–9300.

(14) *Photochromic Materials: Preparation, Properties and Applications*; Tian, H.; Zhang, J., Eds.; Wiley-VCH Verlag GmbH & Co. KGaA: Weinheim, Germany, 2016.

(15) Klajn, R. Spiropyran-Based Dynamic Materials. *Chem. Soc. Rev.* **2014**, *43*, 148–184.

(16) Darwish, T. A.; Tong, Y.; James, M.; Hanley, T. L.; Peng, Q.; Ye, S. Characterizing the Photoinduced Switching Process of a Nitrospiropyran Self-Assembled Monolayer Using In Situ Sum Frequency Generation Spectroscopy. *Langmuir* **2012**, *28*, 13852–13860.

(17) Ivashenko, O.; van Herpt, J. T.; Feringa, B. L.; Rudolf, P.; Browne, W. R. UV/Vis and NIR Light-Responsive Spiropyran Self-Assembled Monolayers. *Langmuir* **2013**, *29*, 4290–4297.

(18) Rosario, R.; Gust, D.; Hayes, M.; Jahnke, F.; Springer, J.; Garcia, A. A. Photon-Modulated Wettability Changes on Spiropyran Coated Surfaces. *Langmuir* **2002**, *18*, 8062–8069.

(19) Bunker, B. C.; Kim, B. I.; Houston, J. E.; Rosario, R.; Garcia, A. A.; Hayes, M.; Gust, D.; Picraux, S. T. Direct Observation of Photo Switching in Tethered Spiropyrans Using the Interfacial Force Microscope. *Nano Lett.* **2003**, *3*, 1723–1727.

(20) Blonder, R.; Levi, S.; Tao, G.; Ben-Dov, I.; Willner, I. Development of Amperometric and Microgravimetric Immunosensors and Reversible Immunosensors Using Antigen and Photoisomerizable Antigen Monolayer Electrodes. *J. Am. Chem. Soc.* **1997**, *119*, 10467–10478.

(21) Kaganer, E.; Pogreb, R.; Davidov, D.; Willner, I. Surface Plasmon Resonance Characterization of Photoswitchable Antigen–Antibody Interactions. *Langmuir* **1999**, *15*, 3920–3923.

(22) Doron, A.; Katz, E.; Tao, G.; Willner, I. Photochemically-, Chemically-, and PH-Controlled Electrochemistry at Functionalized Spiropyran Monolayer Electrodes. *Langmuir* **1997**, *13*, 1783–1790.

(23) Wang, G.; Bohaty, A. K.; Zharov, I.; White, H. S. Photon Gated Transport at the Glass Nanopore Electrode. *J. Am. Chem. Soc.* **2006**, *128*, 13553–13558.

(24) Riskin, M.; Katz, E.; Gutkin, V.; Willner, I. Photochemically Controlled Electrochemical Deposition and Dissolution of Ag 0 Nanoclusters on Au Electrode Surfaces. *Langmuir* **2006**, *22*, 10483–10489.

(25) Riskin, M.; Willner, I. Coupled Electrochemical/Photochemical Patterning and Erasure of Ag 0 Nanoclusters on Au Surfaces. *Langmuir* **2009**, *25*, 13900–13905.

(26) Riskin, M.; Gutkin, V.; Felner, I.; Willner, I. Photochemical and Electrochemical Encoding of Erasable Magnetic Patterns. *Angew. Chem., Int. Ed.* **2008**, *47*, 4416–4420.

(27) Vlassiouk, I.; Park, C.-D.; Vail, S. A.; Gust, D.; Smirnov, S. Control of Nanopore Wetting by a Photochromic Spiropyran: A Light-Controlled Valve and Electrical Switch. *Nano Lett.* **2006**, *6*, 1013–1017.

(28) Vlassiouk, I.; Rios, F.; Vail, S. A.; Gust, D.; Smirnov, S. Electrical Conductance of Hydrophobic Membranes or What Happens below the Surface. *Langmuir* **2007**, *23*, 7784–7792.

(29) Samanta, S.; Locklin, J. Formation of Photochromic Spiropyran Polymer Brushes via Surface-Initiated, Ring-Opening Metathesis Polymerization: Reversible Photocontrol of Wetting Behavior and Solvent Dependent Morphology Changes. *Langmuir* **2008**, *24*, 9558–9565.

(30) Willner, I.; Blonder, R. Patterning of Surfaces by Photoisomerizable Antibody-Antigen Monolayers. *Thin Solid Films* **1995**, *266*, 254–257.

(31) Wen, G.; Yan, J.; Zhou, Y.; Zhang, D.; Mao, L.; Zhu, D. Photomodulation of the Electrode Potential of a Photochromic Spiropyran-Modified Au Electrode in the Presence of Zn<sup>2+</sup>: A New Molecular Switch Based on the Electronic Transduction of the Optical Signals. *Chem. Commun.* **2006**, *0*, 3016–3018.

(32) Rosario, R.; Gust, D.; Hayes, M.; Springer, J.; Garcia, A. A. Solvatochromic Study of the Microenvironment of Surface-Bound Spiropyrans. *Langmuir* **2003**, *19*, 8801–8806.

(33) Gorelik, S.; Hongyan, S.; Lear, M. J.; Hobley, J. Transient Brewster Angle Reflectometry of Spiropyran Monolayers. *Photochem. Photobiol. Sci.* **2010**, *9*, 141–151.

(34) Joseph, G.; Pichardo, J.; Chen, G. Reversible Photo-/Thermoresponsive Structured Polymer Surfaces Modified with a Spirobenzopyran-Containing Copolymer for Tunable Wettability. *Analyst* **2010**, *135*, 2303.

(35) Shiraishi, Y.; Tanaka, K.; Shirakawa, E.; Sugano, Y.; Ichikawa, S.; Tanaka, S.; Hirai, T. Light-Triggered Self-Assembly of Gold Nanoparticles Based on Photoisomerization of Spirothiopyran. *Angew. Chem., Int. Ed.* **2013**, *52*, 8304–8308.

(36) Shiraishi, Y.; Tanaka, H.; Sakamoto, H.; Ichikawa, S.; Hirai, T. Amino-Substituted Spirothiopyran as an Initiator for Self-Assembly of Gold Nanoparticles. *RSC Adv.* **2015**, *5*, 77572–77580.

(37) Liu, Z.; Liu, T.; Lin, Q.; Bao, C.; Zhu, L. Sequential Control over Thiol Click Chemistry by a Reversibly Photoactivated Thiol Mechanism of Spirothiopyran. *Angew. Chem., Int. Ed.* **2015**, *54*, 174–178.

(38) Zhang, H.; Gao, F.; Cao, X.; Li, Y.; Xu, Y.; Weng, W.; Boulatov, R. Mechanochromism and Mechanical-Force-Triggered Cross-Linking from a Single Reactive Moiety Incorporated into Polymer Chains. *Angew. Chem., Int. Ed.* **2016**, *55*, 3040–3044.

(39) Vijayamohanan, H.; Palermo, E. F.; Ullal, C. K. Spirothiopyran-Based Reversibly Saturable Photoresist. *Chem. Mater.* **2017**, *29*, 4754–4760.

(40) El-Faham, A.; Albericio, F. Peptide Coupling Reagents, More than a Letter Soup. *Chem. Rev.* **2011**, *111*, 6557–6602.

(41) Wu, Y.; Sasaki, T.; Kazushi, K.; Seo, T.; Sakurai, K. Interactions between Spiropyrans and Room-Temperature Ionic Liquids: Photochromism and Solvatochromism. *J. Phys. Chem. B* **2008**, *112*, 7530–7536.

(42) Smith, E. A.; Chen, W. How to Prevent the Loss of Surface Functionality Derived from Aminosilanes. *Langmuir* **2008**, *24*, 12405–12409.

(43) Valeur, E.; Bradley, M. Amide Bond Formation: Beyond the Myth of Coupling Reagents. *Chem. Soc. Rev.* **2009**, *38*, 606–631.

(44) Shircliff, R. A.; Stradins, P.; Moutinho, H.; Fennell, J.; Ghirardi, M. L.; Cowley, S. W.; Branz, H. M.; Martin, I. T. Angle-Resolved XPS Analysis and Characterization of Monolayer and Multilayer Silane Films for DNA Coupling to Silica. *Langmuir* **2013**, *29*, 4057–4067.

(45) Zhu, M.; Lerum, M. Z.; Chen, W. How To Prepare Reproducible, Homogeneous, and Hydrolytically Stable Aminosilane-Derived Layers on Silica. *Langmuir* **2012**, *28*, 416–423.

(46) Hell, S. W. Strategy for Far-Field Optical Imaging and Writing without Diffraction Limit. *Phys. Lett. A* **2004**, *326*, 140–145.

(47) Santos, C. S.; Miller, A. C.; Pace, T. C. S.; Morimitsu, K.; Bohne, C. Photochromism of a Spiropyran and a Diarylethene in Bile Salt Aggregates in Aqueous Solution. *Langmuir* **2014**, *30*, 11319–11328.

(48) Zhou, J.-W.; Li, Y.-T.; Song, X.-Q. Investigation of the Chelation of a Photochromic Spiropyran with Cu(II). *J. Photochem. Photobiol. A* **1995**, *87*, 37–42.

(49) Hoyle, C. E.; Bowman, C. N. Thiol-Ene Click Chemistry. *Angew. Chem., Int. Ed. Engl.* **2010**, *49*, 1540–1573.